

Central European Journal of Chemistry

Mechanical, thermal and surface properties of polyacrylamide/dextran semi-interpenetrating network hydrogels tuned by the synthesis temperature

Research Article

Maria V. Dinu, Maria Cazacu, Ecaterina S. Drăgan*

"Petru Poni" Institute of Macromolecular Chemistry, 700487 Iasi, Romania

Received 4 June 2012; Accepted 3 October 2012

Abstract: The mechanical, rheological, thermal, and surface behaviors of three polyacrylamide/dextran (PAAm/Dx) semi-interpenetrating polymer network (semi-IPN) hydrogels, prepared at 22°C, 5°C and -18°C, were investigated. The results were compared with those obtained on cross-linked PAAm without Dx synthesized under the same conditions. Hydrogels prepared at the lowest temperature were the most mechanically stable. The thermal stability of the semi-IPN hydrogels is slightly lower than the corresponding PAAm gels, irrespective of preparation temperature. The water vapor sorption capacity depended on the presence of Dx as well as preparation temperature, which determines the network morphology.

Keywords: Semi-interpenetrating polymer networks • Rheological properties • Thermostability • Water vapor sorption © Versita Sp. z o.o.

1. Introduction

Biocompatible polymer based hydrogels are interesting biomaterials used in controlled drug release devices, tissue engineering, biosensors, artificial muscles, bioseparations, etc. [1-5] due to their ability to mimic body tissue and to respond to external stimuli. However, they show poor mechanical characteristics and slow response. Strategies to improve performance include formation of semi-interpenetrating polymer networks (semi-IPN), construction of interconnected pore structures by cryogelation, embedding clay minerals to obtain organic-inorganic composite hydrogels, etc. [2-4,6-12]. Materials with a broad spectrum of micro-morphologies and properties can be prepared [1]; properties such as swelling, permeation, mechanical, optical, and surface characteristics can be varied for applications from biotechnology to environmental protection [13-15].

Semi-IPN hydrogels are typically produced in a "single step" by synthesis of a hydrophilic polymer matrix around an entrapped water soluble polymer [6,7,9,10-12,16];

alternatively, they are prepared by selective cross-linking of one polymer in a polymer blend [7,17].

In cryogelation soluble monomers, initiator, and polymer are expelled from the ice and concentrated in the liquid channels between ice crystals. Cross-linking polymerization occurs in these channels, the ice crystals acting as a template. Thawing leaves a system with large and interconnected pores called a cryogel. These possesses tissue-like elasticity, withstand high levels of elongation and torsion, and absorb water very rapidly [6,8,9,18-20]. Cryogelation has been used to produce scaffolds with controlled internal microarchitecture by cross-linking two polysaccharides [21].

Poly(acrylamide) (PAAm) is widely used due to its affinity for proteins and other biomolecules. Its amide groups allow further reaction [10-12]. The addition of dextran (Dx, a hydrophilic, biocompatible, and biodegradable linear α -1,6-linked D-glucopyranose polymer) provides a material with new properties. Dextran based hydrogels have been used as carriers for controlled release of antidiabetics, antibiotics,

anticancer drugs, peptides and enzymes [22-25]. For example, acyclovir, an antiviral drug with limited water solubility, has been successfully encapsulated into semi-IPN microspheres of acrylamide grafted on dextran (AAm-g-Dx) and chitosan (CS) by varying the AAm-g-Dx / CS ratio and the amount of glutaraldehyde [22].

Preparation of some novel semi-IPN composite hydrogels based on PAAm and Dx at 22°C, 5°C and -18°C has been recently reported [6]. These rod-shaped gels have been characterized by FTIR spectroscopy, scanning electron microscopy (SEM), differential scanning calorimetry, and their swelling behavior. The results were compared with those obtained on a PAAm network without dextran. The gel swelling ratio is enhanced by Dx, and by conducting the polymerization at -18°C. Semi-IPNs with interconnected pores and superfast-response were obtained [6].

Better understanding of the structure-property relationship is essential to optimize the composition, preparation and processing of materials tailored to specific requirements [2]. Therefore we have extended the study of these composite gels to disks and rods to examine their mechanical and rheological properties as well as their thermostability. Dynamic water vapor sorption analysis was also performed to evaluate surface properties. SEM images of the disks showed their morphology.

2. Experimental procedure

2.1. Materials

Dextran (Dx) (100 kDa) from Leuconostoc mesenteroides was purchased from Sigma-Aldrich and used as received. Acrylamide (AAm, Fluka), N,N'-methylenebis(acrylamide) (BAAm, Sigma), ammonium persulfate (APS, Sigma-Aldrich), and N,N,N',N'-tetramethylethylenediamine (TEMED, Sigma-Aldrich) were used as received. All reagents were of analytical grade or the highest purity available.

2.2. Semi-IPN hydrogel preparation

Semi-IPN hydrogels based on PAAm and Dx were prepared by free radical cross-linking copolymerization in aqueous solution at three temperatures ($T_{prep} = 22$, 5, or -18°C) as reported [6]. The initial concentration of the monomers (AAm+BAAm = C_0) and the cross-linker ratio (X = molar ratio of cross-linker BAAm to monomer AAm) were kept constant ($C_0 = 5$ % w/w; X = 1:80). Stock solutions of APS (0.2 g per 25 mL) and TEMED (0.625 mL per 25 mL) were the redox initiator.

PAAm/Dx semi-IPN hydrogels were prepared at 22°C and 5°C as follows: 0.4868 g AAm, 7 mL Dx aqueous solution (1% w/w), 1 mL BAAm (0.33 g per 25 mL) and 1 mL TEMED stock aqueous solution were first mixed in a 10 mL flask. The solution was purged with nitrogen for 20 min, then 1 mL of APS stock solution was added and the mixture further stirred about 20 sec. Portions (1 mL) were transferred to 4 mm syringes to obtain rod-shaped gels or to 60 mm Petri dishes for disks. The syringes or dishes were sealed, immersed in a thermostat bath at $\rm T_{prep}$ and the polymerization proceeded for one day.

The procedure at $T_{prep} = -18^{\circ}C$ differs slightly. The AAm, Dx, BAAm, and TEMED solutions were mixed as above, but this solution was kept at 0°C in an icewater bath while purged with nitrogen, the APS solution added, and the mixture stirred. This diminished the time necessary to reach -18°C [18]. The solution was then treated as above except a -18°C freezer replaced the constant temperature bath. At -18°C, 10 mL of solution in syringes or petri dishes was frozen in 10 min, while the onset of gelation at X = 1/80 occurred within 30 min. Reaction containers of the same volume and shape were used to obtain reproducible heating or cooling patterns. After polymerization the gels were repeatedly soaked in a large excess of water to wash out soluble polymers, unreacted monomers and the initiator. The swollen rods and disks were used for mechanical measurements. For thermogravimetric analysis and water vapor sorption tests, the swollen rods were carefully deswollen in a series of water-acetone mixtures with increasing acetone contents (vol.%), as follows: 20% (3 h) → $40\% (3 \text{ h}) \rightarrow 60\% (3 \text{ h}) \rightarrow 80\% (3 \text{ h}) \rightarrow 100\% (12 \text{ h}).$ This solvent exchange facilitated final drying at 40°C to constant weight.

Reference samples of cross-linked PAAm without dextran were prepared as above.

2.3. Equipment and procedures for semi-IPN hydrogel characterization

2.3.1. Morphological analysis

The surface morphology and internal structure of the dried semi-IPN hydrogels were observed on a Quanta 200 Environmental Scanning Electron Microscope (ESEM), operating in low vacuum mode at 30 kV with secondary electrons. Disks were frozen in liquid nitrogen and freeze dried in a Martin Christ ALPHA 1-2LD lyophilizer (24 h at -57°C and 0.045 mbar). Samples were cross-sectioned with a sharp blade to reveal the internal structures. The average pore diameter and wall thickness were determined from the SEM photographs using the ACD Photo Editor v3.1 image analysis program. At least 40 pores were measured per sample.

2.3.2. Mechanical-rheological measurements

Uniaxial compression (stress-strain) tests were performed on equilibrium swollen rods in a controlled temperature room (21 \pm 0.5°C). The stress–strain isotherms were measured with a Physik M-150.11 universal materials tester [26]. Briefly, a 5 - 6 mm diameter cylindrical swollen gel sample 10 mm long was placed on a digital balance (Sartorius BP221S, readability and reproducibility: 0.1 mg). After taring, a load was vertically transmitted to the gel through a rod fitted with a PTFE end-plate.

The compressional force (F) was calculated from the balance reading, m:

$$F = m \cdot q \tag{1}$$

where g is the gravitational acceleration. The resulting deformation (ΔI) was:

$$\Delta I = I_0 - I \tag{2}$$

where I_0 and I are the initial and deformed lengths. After 20 s relaxation the latter was measured with a digital comparator (IDC Digimatic Indicator 543-262, Mitutoyo Co.) sensitive to 10^{-3} mm. The measurements were conducted up to about 15% compression.

The deformation ratio α was:

$$\alpha = 1 - \frac{\Delta I}{I_0} \tag{3}$$

and the stress f:

$$f = \frac{F}{\Delta} \tag{4}$$

where A is the initial cross-sectional area:

$$A = \pi r_0^2 \tag{5}$$

and r_o is the initial radius. The modulus relative standard deviations were less than 3%.

Rheological measurements (oscillatory shear) on equilibrium swollen disks provide a quantitative characterization of the viscoelastic properties [27]. The response was determined at constant deformation (γ) during a frequency sweep (ω). Viscoelasticity causes a phase shift (δ). If the deformation does not exceed the linear viscoelastic region, nondestructive characterization is possible and the network parameters can be determined [27,28].

The complex shear modulus (G^*) is the ratio of maximum shear stress (σ_o) to maximum deformation (γ_o) , incorporating the phase shift (δ) :

$$G^* = \frac{\sigma_o}{\gamma_o} e^{i\delta} = G' + i \cdot G''$$
 (6)

where G' is the storage modulus (elastic energy stored) and G'' is the loss modulus (viscous dissipation) [29]. The complex dynamic viscosity, $|\eta^*|$ is:

$$\left|\eta^*\right| = \left[\left(\eta'\right)^2 + \left(\frac{G'}{\omega}\right)^2\right]^{\frac{1}{2}} \tag{7}$$

where η' is the dynamic viscosity.

Rheology was measured using a HAAKE Mars II RheoScope 1 (Thermo Scientific) with parallel plate geometry (\emptyset = 60 mm) and a 1 mm gap. A Peltier plate maintained the temperature at 25°C. The samples were carefully loaded between the plates and the excess hydrogel removed to ensure a cylindrical contact region. All measurements were carried out in the range ω = 0.5 – 100 rad s⁻¹ and in the experimentally determined linear viscoelastic region (γ = 0.005%), where G' and G" are independent of strain. A force of 0.3 N was applied normal to the sample surface to avoid gel slippage from the Peltier plate and water release from the -18°C gels. This resulted in slight sample compression. This setup is comparable to other works [30-32].

2.3.3. Thermogravimetric analysis

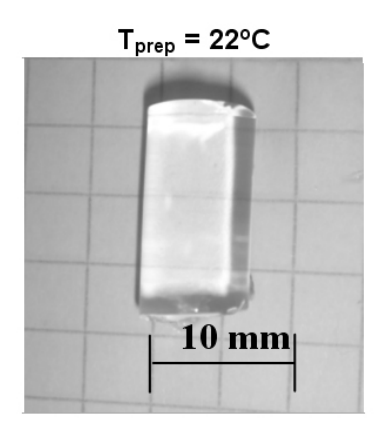
Thermogravimetric analysis (TGA) was performed on 3 – 5 mg samples from 25 to 700 °C at 10 °C min⁻¹ under nitrogen flow (20 cm³ min⁻¹) with a Mettler Toledo TGA/ SDTA 851.

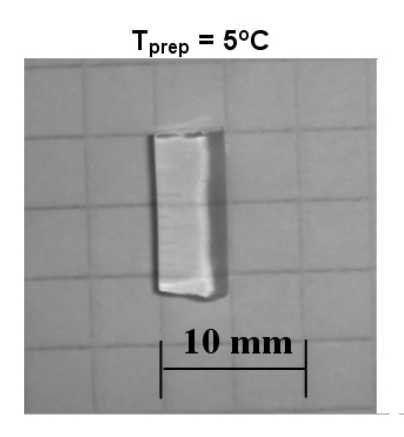
2.3.4. Water vapor sorption capacity

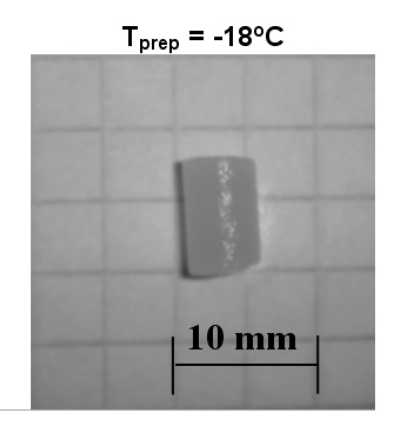
Samples were initially dried to constant weight at 25° C in flowing nitrogen (250 mL min^{-1}) at RH < 1%. Dynamic water vapor sorption was measured using the IGAsorp gravimetric analyzer (Hiden Analytical, Warrington (UK). A microbalance measures the weight change as the sample chamber humidity is changed at constant temperature. Measurements were performed at 25° C and the relative humidity (RH) was increased from 0 – 90% in 10% steps with a 50 - 60 min equilibrium time. Step decreases (10% from 90 - 0%) gave desorption isotherms. A program with 5% humidity steps between 0 and 40% RH and 10% steps between 40 and 90% RH was used to determine the BET surface.

3. Results and discussion

Different shapes of semi-IPN hydrogels have been synthesized by free-radical polymerization at 22°C, 5°C and -18°C, with Dx as physically entrapped









 $T_{prep} = 22^{\circ}C$

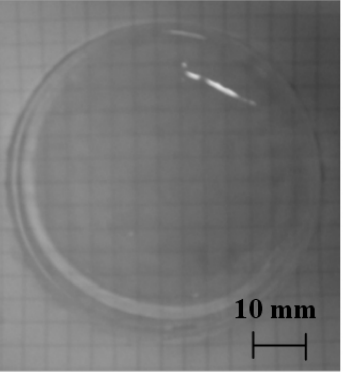




Figure 1. Pictures of PAAm/Dx semi-IPN hydrogels in swollen state prepared in the shape of rods (A) and disks (B).

polymer, AAm as monomer, and BAAm as crosslinker [6]. The gel preparation temperature and Dx presence were key factors controlling the porous structure of the networks. During polymerization, the Dx chains inter-diffuse and get physically entangled with the PAAm 3D network, yielding a semi-IPN hydrogel.

This work is here extended to evaluate the effects of synthesis temperature and the presence of Dx on the mechanical, rheological, thermal, and surface properties.

Optical images of the swollen PAAm/Dx gels prepared as rods and disks are presented in Fig. 1.

The gels formed at -18°C were opaque, indicating separate submicrometer to micrometer domains, while those formed at 22°C or 5°C were semi-transparent with a smooth slippery surface. These differences correspond to different swelling behaviors. In the previous work [6], the swelling ratios of rod-shaped PAAm/Dx gels were 46.68 g g⁻¹, 35.04 g g⁻¹ and 28.25 g g⁻¹ for 22, 5 and -18°C gels. For the disk-shaped gels the swelling ratios were very similar.

Fig. 2 shows SEM images (1000X) of lyophilized hydrogel disks.

The porosity of semi-IPN hydrogels has been reported [6,33,34]. Fig. 2A shows the irregular assembly of spherical pores (36 ± 3 µm) of a 22°C hydrogel. Fig. 2B shows the same morphology in the 5°C hydrogel $(35 \pm 3 \mu m)$. Gels prepared at T > 0°C are porous due to physical entanglement of Dx chains within the 3D PAAm network. This improves the mechanical stability because the pores cannot collapse during deswelling or drying. Decrease of the preparation temperature to -18°C gave a heterogeneous microstructure consisting of interconnected 80 ± 5 µm polyhedral pores (Fig. 2C). As Fig. 2 shows, the main change in morphology when the preparation temperature decreased from 22 to -18°C is an increase in average pore size. At -18°C the ice crystals act as porogen during gelation, leading to a porous architecture with interconnected pores. The thickness of the pore walls was $2.5 \pm 0.5 \mu m$, $3 \pm 0.5 \mu m$, and $12 \pm 2 \mu m$ at preparation temperatures of 22, 5 and -18°C.

10 mm

3.1. Mechanical and rheological properties

The mechanical properties of equilibrium swollen hydrogels were evaluated by uniaxial compression and rheological measurements. Uniaxial compression

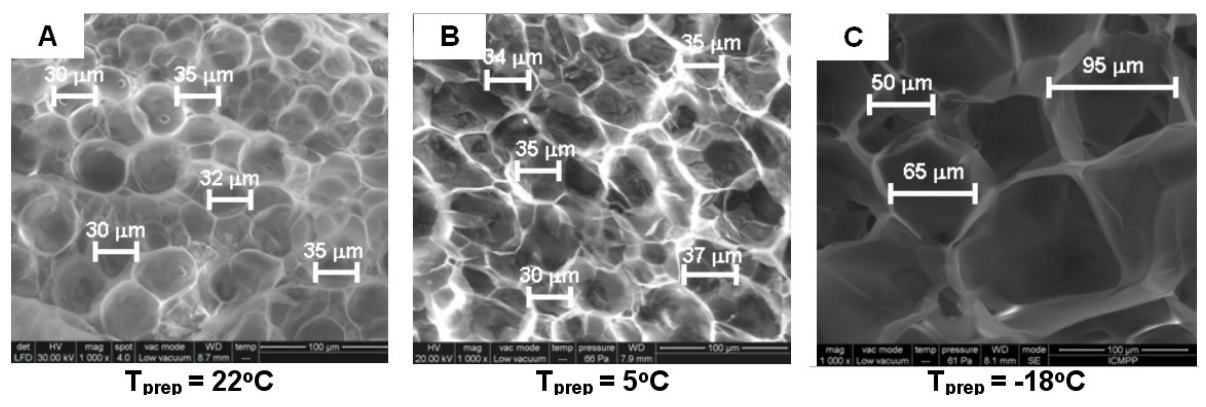


Figure 2. SEM images of the PAAm/Dx semi-IPN hydrogel disks prepared at 22°C (A), 5°C (B), -18°C (C). The scaling bars are 100 µm. Mag. = 1000x.

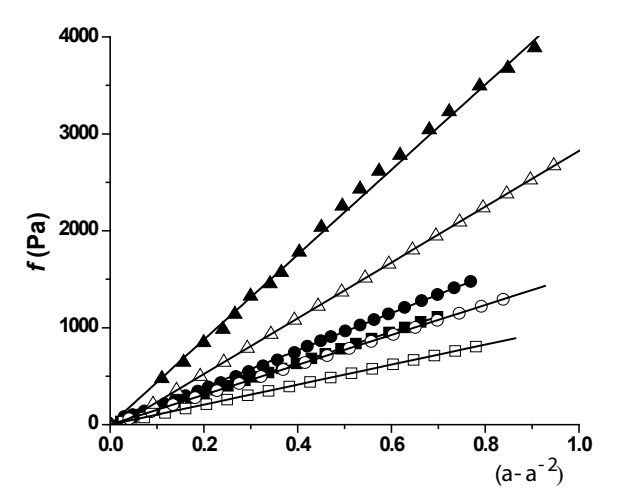


Figure 3. Typical stress-strain data for PAAm hydrogels prepared at 22°C (□), 5°C (○) and -18°C (Δ) and for PAAm/Dx semi-IPN hydrogels prepared at 22°C (■), 5°C (●) and -18°C (▲).

Table 1. Elastic modulus for PAAm/Dx semi-IPN hydrogels prepared at three temperatures with a cross-linker ratio of 1:80.

Sample code	T _{prep} (°C)	Elastic modulus, G (Pa)
PAAm_22	22	1031
PAAm_5 PAAm18	5 -18	1544 2879
PAAm/Dx_22	22	1595
PAAm/Dx_5 PAAm/Dx -18	5 -18	1918 4384

tests the stiffness of a material and describes its elastic deformation along the axis on which forces are applied. The elastic modulus (G) is the stress-strain curve slope in the elastic deformation region [26]. On the other hand, rheology examines viscoelastic and shear behavior. A sinusoidal stress is applied and the strain is measured, allowing one to determine the complex modulus (G^*) [29].

For uniaxial deformation, the statistical theory of rubber elasticity for Gaussian chains gives Eq. 8 [35]:

$$f = G(\alpha - \alpha^{-2}) \tag{8}$$

Uniaxial compression measurements were performed on rod-shaped equilibrium swollen hydrogels. At small compressions deviation from linearity was observed in all samples. This was attributed to the imperfect geometry of the sample surface, which decreases the contact area between the PTFE plate and sample at low compression and results in relatively high deformation at low stress. To correct this, the data at very low strain were discarded. The linear portion of the curve was extrapolated to $-(\alpha - \alpha^2)$ at f = 0, from which the corrected initial length was computed and the deformation ratios determined. The corrected data are shown in Fig. 3. Data for the equilibrium swollen PAAm hydrogels demonstrate the role of Dx.

Table 1 shows the elastic modulus G determined from the slope of f vs. – $(\alpha - \alpha^{-2})$ (Eq. 8 and Fig. 3).

The semi-IPN hydrogels showed higher G values than those without Dx at all preparation temperatures. The 22°C and 5°C gels exhibited elastic moduli of 1595 and 1918 Pa, while those without Dx gave 1031 and 1544 Pa. The -18°C gels were exhibiting more elastic moduli of 4384 Pa for semi-IPN hydrogels and 2879 Pa for the PAAm gels (Table 1). The -18°C gels were very tough and could be stretched by about 100% without cracking. Thus the elastic modulus of the semi-IPN hydrogel networks can be tailored by preparation temperature and Dx addition.

Rheology measures the hydrogel viscoelastic properties, which often link formulation and processing with performance. These properties strongly correlate with the microstructure and are useful in controlling performance [36].

Figs. 4, 5 and 6 show the relationships of G', G'' and $|\eta^*|$ with applied oscillatory frequency.

The storage modulus was higher than the loss modulus (G' > G''), over the whole frequency range: elasticity dominates viscosity and the swollen samples

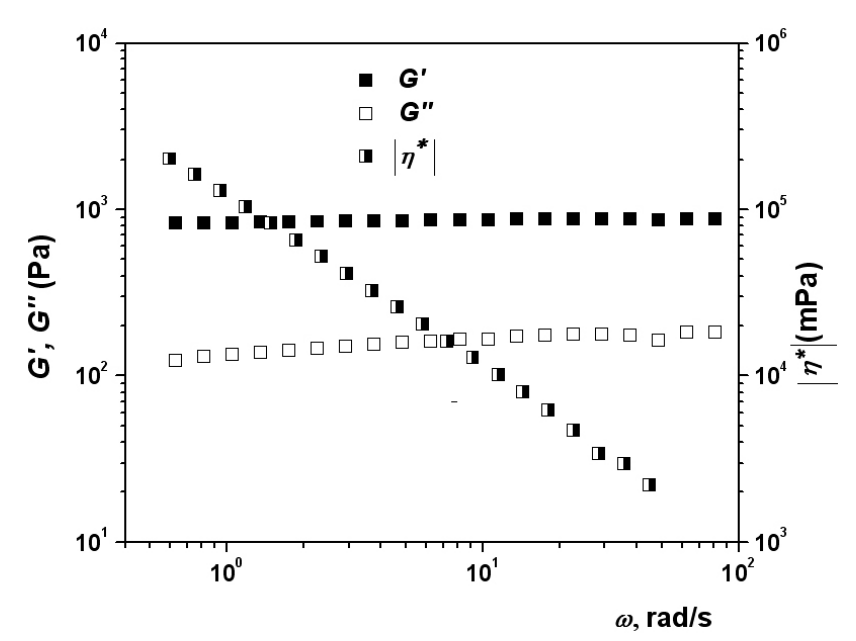


Figure 4. Angular frequency dependence of G', G'' and $|\eta^*|$ for PAAm/Dx semi-IPN gels prepared at 22°C.

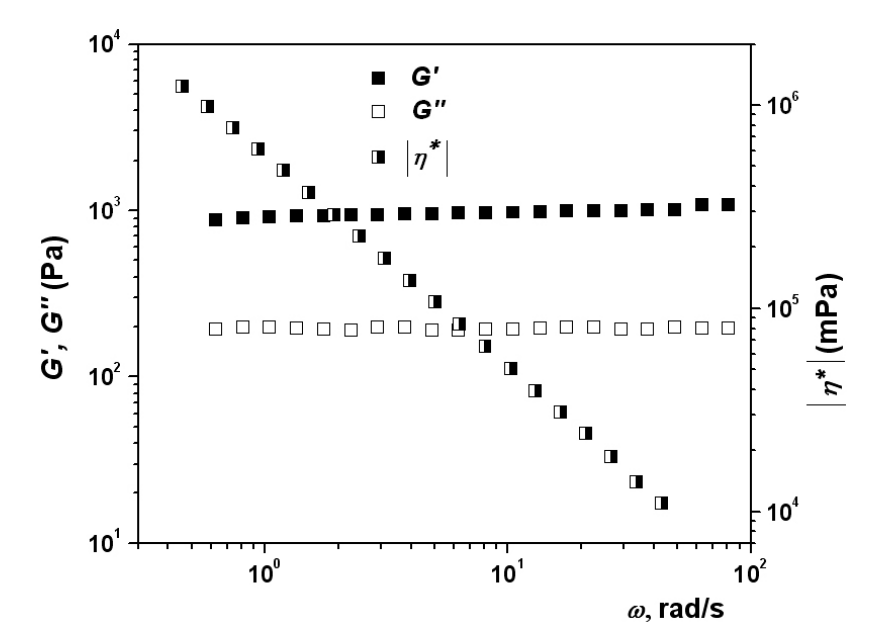


Figure 5. Angular frequency dependence of G', G'' and $|\eta^*|$ for PAAm/Dx semi-IPN gels prepared at 5°C.

are rigid. Moreover, the limiting values of G' and G'' at $\omega = 0$ differ and were greater than zero, also indicating gel-like structures [36].

Semi-IPN gels prepared at -18°C were more elastic, with storage modulus of 1600 Pa, while for the 22°C and 5°C gels it was 850 and 968 Pa. (Fig. 6 compared with Figs. 4 and 5). The improved elasticity of -18°C gels comes from cryogelation, when the polymerization takes place in the non-frozen regions where the monomers are concentrated, unlike 22 or 5°C hydrogels when polymerization occurs in

the whole solution. The semi-IPN gel stability was also improved by synthesis below the solution freezing point; G' was about 30 times G''. For 22°C and 5°C gels the ratios were 7 and 5 (Fig. 6 compared with Figs. 4 and 5).

Figs. 4, 5 and 6 show that the complex viscosity decreased linearly with applied frequency: typical behavior for true gels such as the cross-linked carboxymethyl cassava starch reported by Lawal *et al.* [28]. The complex viscosity increased with decreasing preparation temperature.

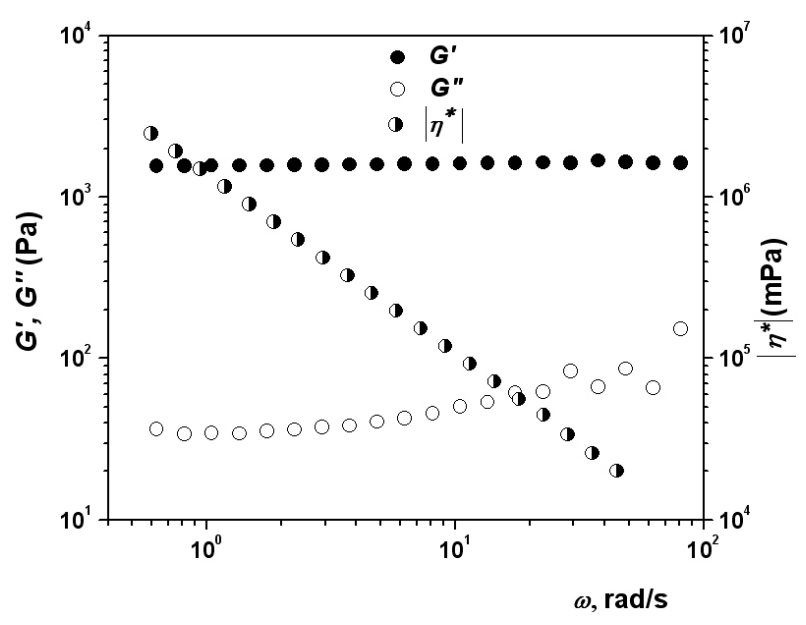


Figure 6. Angular frequency dependence of G', G'' and $|\eta^*|$ for PAAm/Dx semi-IPN gels prepared at -18°C.

The elastic modulus values obtained by uniaxial compression and rheological tests are not comparable because different deformational stress was applied and different shapes were used.

3.2. Thermogravimetric analysis

The thermal stability of semi-IPN hydrogels strongly depends on the polymer matrix structure and trapping mode, being higher [37-39] or lower [40-42] than that of the polymer itself. The thermal behavior of the PAAm/Dx semi-IPN gels was compared to that of the corresponding PAAm gels and Dx. The thermogravimetric (TG) curves and the differential weight loss (DTG) curves for 22°C and -18°C PAAm/Dx gels and PAAm gels compared with Dx are presented in the supplementary material and summarized in Table 2.

Dx decreased the PAAm/Dx gel thermal stability compared to the corresponding PAAm gels, indicating that the Dx chains interdiffuse and are physically entangled in the 3-dimensional PAAm network (no covalent bonds form between Dx and PAAm). This behavior has been reported for other composite hydrogels [40,42]. The gels' thermal stability did not depend on preparation temperature.

Thermal decomposition occurs in two stages for Dx and three stages for PAAm/Dx and PAAm gels, irrespective of preparation temperature. The first weight loss is attributed to loss of water and other volatiles. The lower second stage $T_{\mbox{\tiny onset}}$ for the PAAm/Dx gels than the PAAm gels is attributed to Dx chain degradation, which has $T_{\mbox{\tiny onset}}$ of 220°C. PAAm/Dx gels lost more weight in the third stage as the cross-linked PAAm matrix (main

component) decomposes mainly at higher temperatures. Dx in the gels increased the final char mass.

3.3. Sorption isotherms

Many of the properties useful for medical and applications from microelectronics to adhesives and coatings depend on moisture sorption and water swelling [43]. Hydrogels are cross-linked polymers able to absorb substantial amounts of water and softening without dissolving [7,44]. With their biocompatibility, this makes them important for medical applications as tissue scaffolds, devices for controlled drug delivery, contact lenses, etc. [45].

Kinetic curves depicting time variation of mass and relative humidity in the dynamic vapor sorption (DVS) experiment are shown in Fig. 7.

Fig. 8 shows that the isotherm shape is mainly influenced by the preparation technique (implicitly by morphology) and to a lesser extent by Dx presence. Similar behavior was observed for the 5 and 22°C samples. However, while the isotherms for hydrogels with/without Dx prepared at T > 0°C fall into IUPAC classification III, indicating weak water affinity, the cryogel isotherms are type II with increased water affinity. Both types are characteristic of macroporous adsorbents.

Fig. 8 shows that up to 75% RH all isotherms show hysteresis due to interactions of water sorbed into the bulk [46], swelling the adsorbent. In many cases the deformed structure does not relax even when the water has been removed by outgassing at high temperature, and the original properties are only recovered after long annealing [47].

Table 2. Thermogravimetric characteristics of PAAm/Dx semi-IPN gels, PAAm gels compared with those of Dx.

Sample code	Stage	^a T _{onset} , ∘C	bT _{peak} , ∘C	° W, %	^d M _{resid} , %
PAAm/Dx_22	I	54	72	13.2	22.61
	II	248	272	19.85	
	III	370	387	44.34	
PAAm_22	1	53	76	12.2	18.36
	II	266	327	14.25	
	III	365	389	55.19	
PAAm/Dx_5	1	54	79	13.23	28.98
	II	252	273	17.67	
	III	363	392	40.12	
PAAm_5	1	53	74	13.28	18.51
	II	263	296	14.71	
	III	356	389	53.50	
PAAm/Dx18	1	55	75	13.69	25.60
	II	235	269	21.2	
	III	363	391	39.51	
PAAm18	1	51	79	13.19	18.61
	II	274	300	14.01	
	III	353	385	54.19	
Dx	1	53	82	9.06	39.86
	II	220	225	51.08	

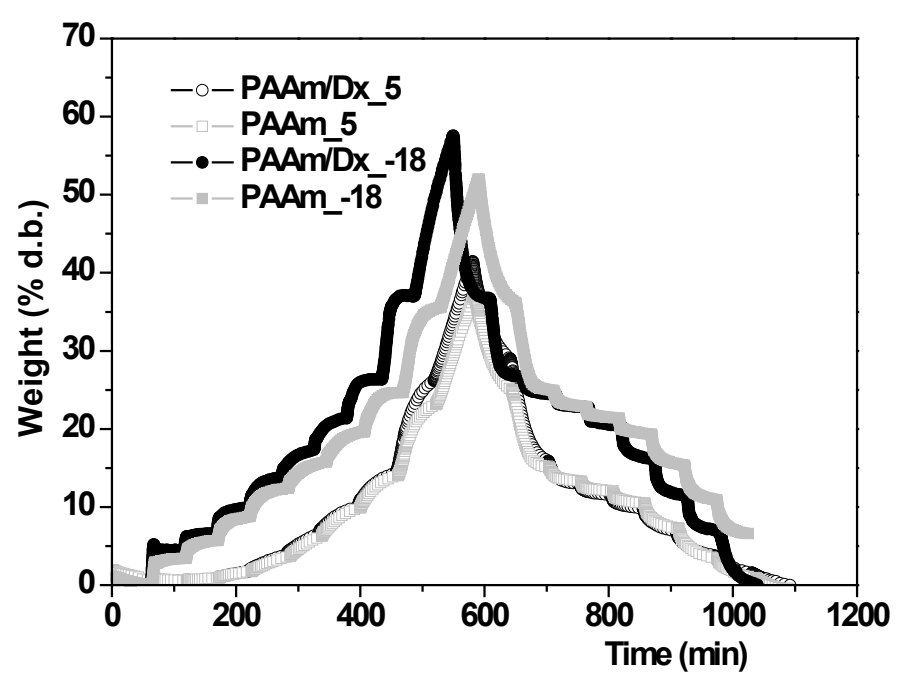


Figure 7. Water sorption-desorption kinetics of PAAm/Dx semi-IPN gels and PAAm gels prepared at 5°C and -18°C.

^aThe onset temperature of the decomposition.
^bThermal degradation peak temperatures of the decomposition.
^cMass loss in every stage.
^cMass remained after the decomposition process.

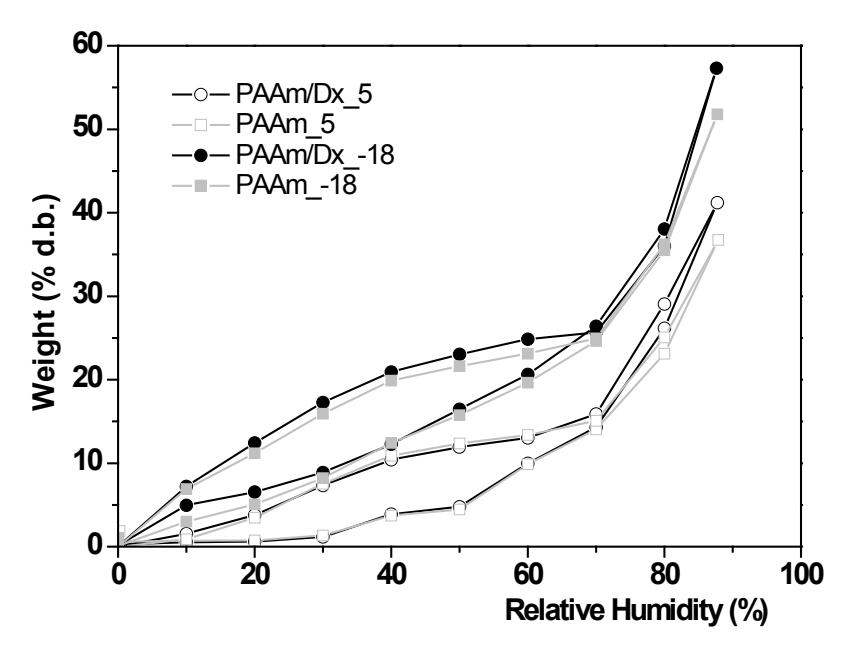


Figure 8. Sorption-desorption isotherms of the PAAm/Dx semi-IPN gels and PAAm gels prepared at 5°C and -18°C.

Table 3. The main surface parameters evaluated based on sorption isotherms.

Sample code	Total water vapors sorption	^a BET _{H2O} data		
	capacity, Weight (% d.b.)	Area (m² g-1)	Monolayer (g g ⁻¹)	
PAAm/Dx_5	41.19	239.34	0.068	
PAAm_5	36.76	248.76	0.070	
PAAm/Dx18	57.32	250.79	0.071	
PAAm18	51.78	328.72	0.093	

BET (Brunauer-Emmett-Teller) [48] data evaluated on the basis of sorption isotherms registered in the relative humidity range 5 - 35%.

The sorption data were used to estimate the BET surface, although the method is limited because the BET model does not consider H-bonding among adsorbed water molecules [48,49]. In addition, compared with the N_2 molecule, water is small and polar and can better penetrate internal surfaces. Higher BET values are generally obtained with water vapor than with N_2 [49-51]. The values for two composite gels and PAAm gels are summarized in Table 3.

Dx presence causes very little change in BET_{H2O} area and water sorption capacity for 5°C gels. Cryogels have the highest BET_{H2O} and water sorption capacity because these parameters are greatly influenced by the morphology, controlled by preparation temperature.

4. Conclusions

By entrapping Dx in a PAAm network at different temperatures, the mechanical, thermal and surface characteristics of semi-IPNs could be varied. The elastic

modulus increased from 1595 Pa for the 22°C PAAm/Dx hydrogel to 1918 Pa for the 5°C PAAm/Dx hydrogel and to 4384 Pa for the hydrogel generated at -18°C. The increased elasticity of the hydrogels is shown by the storage modulus values of 850, 968 and 1600 Pa for the 22, 5 and -18°C semi-IPN gels. Their thermal stability was not significantly affected by the preparation temperature, but it was slightly decreased by Dx incorporation. The total water vapor sorption capacity and BET_{H2O} area depended on the preparation temperature as well as Dx presence. Samples prepared at low temperature showed the highest sorption capacity, which increased only slightly with Dx presence.

Acknowledgements

The financial support of this research by the European Social Fund – "Cristofor I. Simionescu" Postdoctoral Fellowship Programme (ID POSDRU/89/1.5/S/55216), Sectorial Operational Programme Human Resources Development 2007–2013 is gratefully acknowledged.

References

- [1] A. Spanoudaki, D. Fragiadakis, K. Vartzelinikaki, P. Pissis, J.C.R. Hernandez, M.M. Pradas, In: J.P. Blitz, V.M. Gun'ko (Eds.), Surface chemistry in biomedical and environmental science (Springer, Dordrecht, 2006) 229
- [2] D.E. Rodriguez-Felix, C.J. Perez-Martinez, M.M. Castillo-Ortega, M. Perez-Tello, J. Romero-Garcia, A.S. Ledezma-Perez, T. Del Castillo-Castro, F. Rodriguez-Felix, Polym. Bull. 68, 197 (2012)
- [3] C.C. Lin, K.S. Anseth, Pharma. Res. 26, 631 (2009)
- [4] X. Zhong, C. Ji, A.K.L. Chan, S.G. Kazarian, A. Ruys, F. Dehghani, J. Mater. Sci: Mater. Med. 22, 279 (2011)
- [5] J. Michalek, M. Pradny, A. Artyukhov, M. Slouf, K. Smetana Jr., J. Mater. Sci: Mater. Med. 16, 783 (2005)
- [6] M.V. Dinu, M.M. Perju, E.S. Drăgan, Macromol. Chem. Phys. 212, 240 (2011)
- [7] D. Myung, D. Waters, M. Wiseman, P.E. Duhamel, J. Noolandi, C.N. Ta, C.W. Frank, Polym. Adv. Technol. 19, 647 (2008)
- [8] V.I. Lozinsky, Russ. Chem. Bull. Int. Ed. 57, 1015 (2008)
- [9] M.V. Dinu, M.M. Perju, E.S. Drăgan, React. Funct. Polym. 71, 881 (2011)
- [10] E.S. Drăgan, M.M. Perju, M.V. Dinu, Carbohydr. Polym. 88, 270 (2012)
- [11] E.S. Dragan, D.F. Apopei, Chem. Eng. J. 178, 252 (2011)
- [12] E.S. Dragan, M.M. Lazar, M.V. Dinu, F. Doroftei, Chem. Eng. J. 204-206, 198 (2012)
- [13] A.K. Kabiri, H. Omidian, M.J. Zohuriaan-Mehr, S. Doroudiani, Polym. Compos. 32, 277 (2011)
- [14] Y. Yu, X. Chang, H. Ning, S. Zhang, Cent. Eur. J. Chem. 6, 107 (2008)
- [15] Y. Yu, Y. Li, C. Zhu, L. Liu, Cent. Eur. J. Chem. 8, 426 (2010)
- [16] W. Wang, Q. Wang, A. Wang, Macromol. Res. 19, 57 (2011)
- [17] L.H. Sperling, In: D. Klempner, L.H. Sperling, L.A. Utracki (Eds.), Interpenetrating polymer networks (American Chemical Society, Washington, 1994) 3
- [18] M.V. Dinu, M.M. Ozmen, E.S. Drăgan, O. Okay, Polymer 48, 195 (2007)
- [19] H. Kirsebom, D. Topgaard, I. Yu. Galaev, B. Mattiasson, Langmuir 26, 16129 (2010)
- [20] N. Orakdogen, P. Karacan, O. Okay, React. Funct. Polym. 71, 782 (2011)

- [21] A. Tripathi, A. Kumar, Macromol. Biosci. 11, 22 (2011)
- [22] A.P. Rokhade, S.A. Patil, T.M. Aminabhavi, Carbohydr. Polym. 67, 605 (2007)
- [23] Y. Liu, M.B. Chan-Park, Biomaterials 30, 196 (2009)
- [24] R.Y. Cheung, Y. Ying, A.M. Rauth, N. Marcon, X. Yu Wu, Biomaterials 26, 5375 (2005)
- [25] A. Autissier, C. Le Visage, C. Pouzet, F. Chaubet, D. Letourneur, Acta Biomaterialia 6, 3640 (2010)
- [26] C. Sayil, O. Okay, Polymer, 42, 7639 (2001)
- [27] C. Seidel, W.M. Kulicke, C. Heß, B. Hartmann, M.D. Lechner, W. Lazik, Starch/Stärke 56, 157 (2004)
- [28] O.S. Lawal, J. Storz, H. Storz, D. Lohmann, D. Lechner, W.M. Kulicke, Eur. Polym. J. 45, 3399 (2009)
- [29] A. Martinez-Ruvalcaba, E. Chornet, D. Rodrigue, Carbohydr. Polym. 67, 586 (2007)
- [30] P. Petrov, E. Petrova, R. Stamenova, C.B. Tsvetanov, G. Riess, Polymer 47, 6481 (2006)
- [31] X. Yang, Q. Liu, X. Chen, F. Yu, Z. Zhu, Carbohydr. Polym. 73, 401 (2008)
- [32] Q. Zhao, J. Sun, X. Wu, Y. Lin, Soft Matter 7, 4284 (2011)
- [33] J. Chen, M. Liu, H. Liu, L. Ma, C. Gao, S. Zhu, S. Zhang, Chem. Eng. J. 159, 247 (2010)
- [34] T.T. Reddy, A. Takahara, Polymer 50, 3537 (2009)
- [35] L.R.G. Treloar, In: L.R.G. Treloar (Ed.), The elasticity of a molecular network (University Press, Oxford, 1975) 59
- [36] L. Janovák, J. Varga, L. Kemény, I. Dékány, Colloid Polym. Sci. 286, 1575 (2008)
- [37] Y. Liu, Y. Cui, Polym. Int. 60, 1117 (2011)
- [38] Y. Zhou, D. Yang, X. Gao, X. Chen, Q. Xu, F. Lu, J. Nie, Carbohydr. Polym. 75, 293 (2009)
- [39] D.L. Merlin, B. Sivasankar, Eur. Polym. J. 45, 165 (2009)
- [40] M.N. Khalid, F. Agnely, N. Yagoubi, J.L. Grossiord, G. Couarraze, Eur. J. Pharma. Sci. 15, 425 (2002)
- [41] N.B. Milosavljević, N.Z. Milašinović, I.G. Popović, J.M. Filipović, M.T. Krušić Kalagasidis, Polym. Int. 60, 443 (2010)
- [42] K. Burugapalli, D. Bhatia, V. Koul, V. Choudhary, J. Appl. Polym. Sci. 82, 217 (2001)
- [43] S. Chen, J. Hu, H. Zhuo, J. Mat. Sci. 46, 6581 (2011)
- [44] Y.K. Sung, M.S. Jhon, D.E. Gregonis, J.D. Andrade, Polymer (Korea) 8, 123 (1984)
- [45] A. Stathopoulos, P. Klonos, A. Kyritsis, P. Pissis, C. Christodoulides, J.C.M. Rodriguez Hernández,

- M. Pradas, J.L. Gómez Ribelles, Eur. Polym. J. 46, 101 (2010)
- [46] L. Zhou, Master Thesis, University of Minnesota (Minnesota, USA, 2010)
- [47] C.G.V. Burgess, D.H. Everett, S. Nuttall, Pure Appl. Chem. 61, 1845 (1989)
- [48] S. Brunauer, P.H. Emmett, E. Teller, J. Am. Chem. Soc. 60, 309 (1938)
- [49] S.L. Wang, C.T. Johnston, D.L. Bish, J.L. White, S.L. Hem, J. Col.Interf. Sci. 260, 26 (2003)
- [50] L. Czepirski, E. Komorowska-Czepirska, J. Szymońska, Appl. Surf. Sci. 196, 150 (2002)
- [51] Z. Sokołowska, J. Jamroz, P. Bańka, Int. Agrophys. 22, 75 (2008)